Kes 73: A Young Supernova Remnant with an X-ray Bright, Radio-quiet Central Source

E. V. Gotthelf[1]
NASA/Goddard Space Flight Center, Greenbelt, MD 20771

G. Vasisht
California Institute of Technology, MS 105-24, Pasadena, CA 91125

ABSTRACT

We clarify the nature of the small-diameter supernova remnant (SNR) Kes 73 and its central compact source, 1E 1841−045, using X-ray data acquired with the ASCA Observatory. We introduce a spatio-spectral decomposition technique necessary to disentangle the ASCA spectrum of the compact source from the barely resolved shell-type remnant. The source spectrum (1 – 8 keV) is characterized by an absorbed power-law with a photon index $\alpha \simeq 3.4$ and $N_H \simeq 3.0 \times 10^{22}$ cm^{-2}, possibly non-thermal in nature. This bright X-ray source is likely a slowly spinning pulsar, whose detection is reported in our companion paper (Vasisht & Gotthelf 1997). The SNR spectrum is characteristic of a thermal plasma, with kT $\simeq 0.7$ keV, and emission lines typical of a young remnants. The element Mg and possibly O and Ne are found to be over-abundant, qualitatively suggesting an origin from a massive progenitor. We find that Kes 73 is a young ($\lesssim 2000$ yr) type II/Ib SNR containing a neutron star pulsar spinning anomalously slow for its age. Kes 73 is yet another member of a growing class of SNRs containing radio-quiet compact sources with a hard spectral signature.

Subject headings: stars: individual (Kes 73, 1E 1841−045) — stars: neutron — supernova remnants — X-rays: stars

1. Introduction

The supernova remnant Kes 73 is a limb - brightened, shell-type radio remnant $\sim 4'$ in diameter, located along the Galactic plane (G 27.4+0.0). The X-ray remnant is comparable in size to the bright radio shell, but is dominated by localized emission knots, interpreted as clumpy, diffuse emission in the interior, possibly due to fluorescence from reverse shock (Helfand et al.

[1]Also: Universities Space Research Association

1994 using ROSAT HRI images). Centered on the remnant is the unresolved compact X-ray source, 1E 1841−045, discovered with the Einstein Observatory (Kriss et al. 1985). Like the supernova remnants RCW 103 and CTB 109, the radio observations show no evidence for a plerionic component or a localized radio counterpart to 1E 1841−045, with a flux limit $F_{6cm} < 0.6$ mJy (Kriss et al. 1985). An HI absorption-based distance determination shows that Kes 73 lies ~ 7.0 kpc away (Sanbonmatsu & Helfand 1992).

The nature of Kes 73 and in particular, its compact source, has been considered extensively in two earlier studies. Kriss et al. (1985) were unable to distinguish between thermal and non-thermal emission from 1E 1841−045; they suggested as the origin of the emission either a hot thermal neutron star (NS), a crab-like pulsar, a plerionic nebula, or an accretion powered binary. A more recent study by Helfand et al. (1994) reconsidered these possibilities using deep ROSAT HRI pointings. They inferred a hard spectral component for 1E 1841−045, placed a limit on its long term variability of a factor of two change in flux, and suggested an accreting binary origin for the central source.

In this *Letter*, we use the broad-band ASCA X-ray observations of Kes 73 to further clarify its nature. We present a novel technique for isolating the background subtracted spectrum of the central source. We show that the spectrum of 1E 1841−045 is represented by a steep power law, possibly of non-thermal origin, and suggest that Kes 73 is a young ($\lesssim 2000$ yrs) Type II/Ib SNR, the product of a massive progenitor. In our companion paper (Vasisht & Gotthelf, referred herein as GV97) we report our discovery of a 11.8 s periodicity from 1E 1841−045, likely from an anomalous pulsar, the stellar remnant of the supernova explosion. The date and typing of Kes 73 are critical to understand the nature of the pulsar. We present Kes 73 as another member of an emerging class of young thermal remnants which are found to contain a radio-quiet, hard X-ray point source.

2. Observations

ASCA (Tanaka et al. 1994) conducted a two day observation of Kes 73 on 11-12 Oct 1993. In this study, we use data acquired with the two Solid State Imaging Spectrometers (SIS-0 and SIS-1), made available from the public archive. These sensors are sensitive to X-rays in the $0.4 - 10.0$ keV band, with a nominal spectral resolution of 2% at 6 keV ($\sim E^{-1/2}$). The spatial resolution is limited by the X-ray mirrors, whose azimuthally averaged point spread function (PSF) is characterized by a narrow core of FWHM $50''$, and extended wings that result in a half-power diameter of $3'$ (Jalota et al. 1993). The SIS data were acquired in 1-CCD mode, read out every 4 sec, using a combination of FAINT and BRIGHT data modes. The target was centered on the $11' \times 11'$ field-of-view of SIS-0 CCD-1. All data were edited using the standard REV1 screening criteria which resulted in an effective exposure of ~ 34 ksecs per sensor. A description of the data acquired with the other two focal plane instruments is presented in our companion paper (GV97).

The broad-band image of Kes 73 from the combined SIS cameras contains 93 kcounts, with a count rate of 1.38 cps. In Plate 1 we display images of the Kes 73 region in the soft- and hard-band, below and above 2.5 keV, respectively. The images are centered on the point-like source, whose position is consistent with that of 1E 1841−045, to within the formal SIS error circle (Gotthelf 1996). The hard-band image clearly shows the clover-leaf shaped PSF, consistent with an unresolved point source, whereas the soft-band image suggest an additional diffuse structure. The FWHM of the normalized brightness distribution profiles in the two bands are $44''$ (hard) and $108''$ (soft) (see Fig 1). This difference is more apparent in the deconvolved images in the lower panel of Plate 1. These clearly show that the thermal X-ray shell is contained in the soft-band and surrounds the harder, bright compact source. The images have been restored with 50 iterations of the Lucy algorithm (Lucy 1974) to deconvolve the complex shape of the PSF, and are displayed in an identical fashion.

An image of the SNR nebulosity is made by subtracting the compact component from the soft-band image. For this, we used as a model PSF the SIS image of the moderately bright point-like source EX Hydra, normalized by the derived source spectrum (see below) to estimate the relative contribution of the compact source to the total emission below 2.5 keV. The subtracted SIS image closely follows the brightness distribution in the smoothed Rosat HRI image (Plate 1c), reproducing the three areas of enhanced emission. Other features are easily ascribed to differences in the spectral response of the two instruments. See Hwang & Gotthelf (1997) for a discussion on interpreting features in the processed images.

3. Isolating the compact source spectrum

The broad winged ASCA PSF does not allow spatial isolation of the point-source emission from that of the SNR. Instead we adopt a spatio-spectral decomposition method detailed in Wang & Gotthelf (1997) (referred herein as WG97) to separate the spectra of the two components. We then use the decomposed point-source spectrum to: (i) verify and consolidate the fit to the point-source spectrum in the total spectrum of the Kes 73 region (see §4.2) and (ii) compute fluxes and luminosities of the point-source. Below we outline a modified version of the WG97 method, germane to a point source embedded within a SNR shell.

We start with the assumption that the spatial distribution of the Kes 73 emission consists of two components, i.e., a point-source embedded in a diffuse nebula. We then decompose the source spectrum from the underlying nebula (+ background), by simultaneously solving for the source and nebular spectra using the ratio of observed and expected counts in concentric regions; we search for deviations from the radial-average profile centered on the source, from that expected for a point-source.

The original method, discussed in WG97, assumes a uniform background. From the Rosat HRI morphology, we know this is not the case for Kes 73, for which the background consists of both

the thermal-shell emission and the field-background. Therefore, we use the HRI data to estimate a correction factor to a uniform background from the relative counts in the source and nebular region. Our procedure is as follows: (i) We first extract spectra from two annuli centered on the source (see Fig. 1). The first annulus is a small circle ($r = 1\farcm2$) encompassing the central pulsar counts. The second annulus ($1\farcm5 > r \geq 2\farcm7$) is chosen to enclose the bulk of the shell emission. (ii) Next, we compute the expected radial profile for a point-source in these regions from a similar 1-CCD mode observation of EX Hydra. To compensate for the non-uniform SNR distribution, we compute a nebular correction factor using the relative counts per pixel between the center and edge of the projected HRI X-ray nebula (iii) With the above information, we decompose the spectra in the two annuli into a source spectrum and a nebular spectrum using eqns. A2 3-4 of WG97, applied to each spectral channel.

The spectra separated into two unmixed components: a line dominated spectra expected from thermal emission of a shocked SNR shell and a steep power-law continuum spectrum for the compact source. These are shown on Plate 1a & 1b. No coercion or prejudice is used to force the clean separation into the distinct nebula and source spectra. The background subtracted source spectrum (Plate 1a) accounts for the harder (> 2.5 keV) emission and provides an independent absorption measurement. The spectrum is trivially fitted with an absorbed power-law with a photon index $\Gamma = 3.4 \pm 0.3$ and $N_H \simeq 3.0 \pm 0.4 \times 10^{22}$ cm^{-2}. The inferred unabsorbed luminosity is $L_X(1.0 - 10.0 \text{ keV}) \sim 3 \times 10^{35}$ d$_7^2$ erg s^{-1}, for an assumed distance of 7.0 d_7 kpc (see Table 1). The spectral shape ($\propto E^{-2}$) is in accordance with the steep power-law spectra seen in other anomalous X-ray pulsars (see Corbet et al. 1995). We now use this fit to constrain the power-law emission component in the combined fit to the Kes 73 spectrum.

4. The SNR nebula spectrum

The SIS energy spectrum photons were selected from within a circular emission region of radius $\simeq 4'$, limited by the size of the CCD. The broad ASCA PSF makes background estimation extremely difficult, since the source flux from a diffuse object extends over most of the CCD chip. For this analysis, we extract a background spectrum from nearby archival pointings of the Galactic ridge. The resulting background-subtracted spectrum of the shell plus compact source is shown in Fig 2. The line-dominated spectrum, typical of those seen from SNRs, suffers high foreground absorption in the energy range below ~ 1.5 keV. In the energy range spanning $\sim 1 - 10$ keV, we see K-shell emission from highly ionized ions of Mg, Si, S, Ca, and Ar. The identified emission lines and their characteristic parameters are displayed in Table 2.

Collisional ionization equilibrium (Raymond & Smith 1977; Mewe et al. 1985 and references therein) and thermal bremsstrahlung models with Gaussians for line emission, are fit to the spectra. There are large residuals, in either case, in the hard-band (2.5 - 10.0 keV) suggesting an extra emission component. The image analysis, spanning that energy range, clearly demonstrates that this component is mostly emission from the compact source, for which we add a single

power-law to the fit. A bremsstrahlung continuum, with Gaussians and a power-law tail provides the best fit (see Table 1). In contrast, the single temperature Raymond-Smith model with fixed relative metal abundances and a power-law, is a relatively poor fit; it shows large negative residuals mainly near the over-abundant Mg feature, and a relatively large metal abundance of $\simeq 2.0$ cosmic, driven mainly by the strong Si (1.83 keV) feature. In addition, we note excess flux in all our fits, at the lower energy range, $0.5 - 0.9$ keV, which we tentatively ascribe to O and Ne.

5. Discussion

A lower limit on the SNR age can be derived assuming free expansion of the spherical remnant. For a typical maximum velocity of 10^4 km s^{-1} seen in Type II SN, the projected size of Kes 73, $R_s \simeq 4.7\ d_7$ pc, contrains its age to be $\tau_s < 470$ yrs. Since most of the thermal emission is due to shocked matter of electron temperature $kT_e = 0.8$ keV, we compute a shock speed $v_s = (16\mathrm{kT_e}/3\mu\mathrm{m_p})^{1/2} \sim 900$ km s^{-1}. This assumes ion and electron equilibrium behind the shock ($\mu = 0.6$ for cosmic abundances). Inefficient electron heating would result in a larger shock velocity, i.e., $v_s \gtrsim$ 900 km s^{-1}. If we assume that the remnant has entered a well developed Sedov phase, $R_s = 2.5 v_s \tau_s$, and therefore $\tau_s \lesssim 2.2 \times 10^3$ yr. This age is further reduced if the remnant is not fully in Sedov phase. From spectral fitting, the total thermal ($1 - 10$ keV) luminosity of the SNR is $L_X \sim 3 \times 10^{35} d_7^2$ erg s^{-1} (this estimate excludes the uncertain, highly-absorbed emission from O and Ne). The instantaneous power radiated from a shell is $L_s(t) = (16\pi/3) R_s^3(t) n_o^2 \Lambda(T)$, where n_o is the mean pre-shock particle density and $\Lambda(T) = 1.0 \times 10^{-22} T_6^{-0.7} + 2.3 \times 10^{-24} T_6^{0.5}$ erg cm^3 s^{-1} is the cooling function (McCray 1987), and T_6 is the $\mathrm{kT_e}$ in units of 10^6 K. We derive an $n_o \sim 0.8 d_7^{-0.5}$ cm^{-3}. Under the strong-shock assumption the post-shock electron density is ~ 3 cm^{-3}.

Kes 73 is evidently young, with the shocked plasma still ionizing and thus non-equilibrium effects in the ionization balance are important. We determined the diagnostic parameters for the non-equilibrium ionization (NEI) plasma from the line intensity ratios of He-like-Kα to H-like-Kα, as well as, He-like-Kβ to He-like-Kα ionic transitions of individual ions, Si and S in this case. The former ratio is a measure of the ionization degree and is dependent upon both the electron temperature $\mathrm{kT_e}$ and the ionization age n_et, the product of the electron density and time since the gas was last heated by the shock (Itoh 1977). The latter ratio, however, is solely a function of kT_e. The obtained He-like-Kβ to He-like-Kα ratio for Si and S is 0.087 ± 0.015 and 0.089 ± 0.039, respectively. The He-like-Kα to H-like-Kα intensity ratio of Si and S are 22 ± 9 and 15 ± 9, respectively. We measure a $kT_e \simeq 0.75 - 0.90$ keV and $0.71 - 0.97$ keV for Si and S, respectively, assuming a single uniform plasma continuum and a power-law. These are in accordance with the $\mathrm{kT_e}$ derived from the single temperature bremsstrahlung continuum. The ionization parameter was estimated to lie in the range $n_e t \simeq 11.0 - 11.4$ (Masai 1984). Using the post-shock density inferred via normalization to the continuum component, we get $t = \tau_s \sim 1800$ yr. Several independent arguments, therefore, suggest that Kes 73 is a young SNR, ~ 2000 yr-old, as indicated by earlier

studies (Helfand et al. 1994).

We estimate the total mass of the swept-up interstellar gas to be $M_s \simeq 8.8 d_7^3$ $M_\odot$. This corresponds to typical envelop masses ejected in a Type II supernova (progenitor mass $M > 8$ $M_\odot$), suggesting that the SNR dynamics could well still be in a transitional stage between the free expansion and Sedov phases. This notion is qualitatively consistent with the development of a strong reverse shock that can heat the metal-rich gas and cause the diffuse emission to be seen in the SNR interior. Additionally, the detection of strong Mg, Si, S, and Ar emission and perhaps accompanying O and Ne emission suggests ejecta-dominated gas. During their evolution, massive stars are expected to produce large amounts of O-group elements which are ejected during the supernova (Thieleman, Nomoto & Hashimoto 1994; Woosley 1991). These patterns have been observed in the X-ray spectra of O-rich SNR (see Hughes & Singh 1994; Hayashi et al. 1994). Here the emission is highly absorbed and does not permit quantitative estimates of O and Ne emission (although, upper-limits and observed photon excess in the spectral range 0.4 - 1 keV are consistent with abundant O and Ne).

The thermal spectrum of Kes 73 is remarkably similar to that of two young, distant (therefore, high-absorbed) Type II/Ib SNRs, G 11.2−0.3 and RCW 103. The former is a historical SNR (supernova A.D. 386) and hence approximately the same age as Kes 73 (Vasisht et al. 1996). Unlike Kes 73, it contains a weak, but extended hard X-ray plerionic core. RCW 103 is a virtual twin of Kes 73; both have radio-quiet, point-like X-ray sources in their centers, share morphological similarities, while neither shows evidence for a radio or X-ray plerion (see Gotthelf et al. 1997 and refs therein). We infer a minimum energy in particles and nebular magnetic fields in the Kes 73 core to be $E_{min} < 10^{47}$ $d_7^{17/7}$ erg, assuming Crab-like parameters and equipartition between magnetic fields and relativistic particles (Pacholczyk 1970).

The lack of observed plerionic emission can be qualitatively explained in the following manner. If the Kes 73 pulsar has a large dipolar field $B \sim 10^{15}$ G (VG97), a weak plerion is a natural consequence at an age of $\sim 2 \times 10^3$ yr. Such a pulsar loses most of its initial spin energy in a matter of $\sim$ years. The released pulsar wind would immediately suffer strong adiabatic and synchrotron losses. This leads to a bright plerion at an early age ($\sim 10 - 100$ yrs) with subsequent rapid decline in surface brightness. This effect is shown by Bhattacharya (1990) in his paper on the morphology of SNR with central pulsars. He shows that for pulsars with B-fields spanning the range 10^{12} G to 1.5×10^{13} G, the ones with the highest B have the faintest plerions at an elapsed time $t \sim 10^3$ yr. For magnetars, $B \simeq 10^{15}$ G, this rapid decline in surface brightness may be much more pronounced.

Acknowledgements: This research has made use of data obtained through the HEASARC at GSFC. We thank Shri Kulkarni for discussions. GV thanks GSFC for hosting him. EVG's research is supported by NASA. GV's research is supported by NASA and NSF grants.

REFERENCES

Bhattacharya, D. 1990, JAA, 11, 125

Gotthelf, E. V. 1996, ASCA news, no. 4

Gotthelf, E. V., Petre, R., & Hwang, U. 1997, ApJL, submitted.

Hayashi, I., Koyama, K., Ozaki, M., Miyata, E., Tsunemi, H., Hughes, J. P., & Petre, R. 1994, PASJ, 46, L121

Helfand, D. J, Becker, R. H., Hawkins, G. & White, R. L. 1994, ApJ, 434, 627

Hughes, J. P. & Singh. K. P. 1994, ApJ, 422, 126

Hwang, U. & Gotthelf, E. V. 1997, ApJ, 475, 665

Itoh, H. 1977, PASJ, 29, 813

Jalota, L., Gotthelf, E. V. & Zoonermatkermani, S. 1993, Proc. SPIE, 1945, 453.

Kriss, G. A., Becker, R. H., Helfand, D. J. & Canizares, C. J. 1985, ApJ, 288, 703

Lucy, L. 1974, AJ, 79, 745

Masai, K. 1984, Astro. Sp. Sci., 98, 367

McCray, R. 1987 in Spectroscopy of Astrophysical Plasmas, Eds. A. Dalgarno & D. Layzer, Cambridge Univ. Press, 255

Mewe, R., Gronenschild, E. H. B. M. & van den Oord, G. H. J. 1985, A&AS, 62, 197

Pacholczyk, A. G. 1970, in "Radio Astrophysics" Freeman (San Francisco)

Raymond, J. C., & Smith, B. W. 1977 ApJS, 35, 419

Sanbonmatsu, K. Y. & Helfand, D. J. 1992, AJ, 104, 2189

Thielemann, F. K., Nomoto, K. & Hashimoto, M. 1994, in Supernovae, Les Houches, Session 54, eds. S. Bludman, R. Mochkovitch & J. Zinn Justin, Elsevier Sci. Pub., 629

Tanaka, Y., Inoue, H. & Holt, S. S. 1994, PASJ, 46(3), L37

Vasisht, G., Aoki, T., Dotani, T., Kulkarni, S. R. & Nagase, F. 1996, ApJ, 456, L59

Vasisht, G. & Gotthelf, E. V. 1997, ApJ, in press [EDITOR - PLEASE UPDATE]

Wang. Q. D. & Gotthelf. E. V. 1997 ApJ, in press

Woosley, S. E. 1991, in Supernovae, The Tenth Santa Cruz Summer Workshop in Astronomy and Astrophysics, ed. S. E. Woosley (Berlin: Springer), pp 203

Fig. 1. – Radial profiles of Kes 73 in the hard- and soft-bands (above and below 2.5 keV). The hard-band profile is consistent with an unresolved point source, while the soft-band profile indicates additional diffuse emission. The dotted vertical lines indicate the regions used in the spectral decomposition (see §3).

Fig. 2. – The SIS spectrum and model of the Kes 73 region: The upper panel represents a background subtracted pulse-height spectrum of the supernova remnant in the entire region ($r \lesssim 4'$), and the best model function of a thermal plasma consisting of a bremsstrahlung continuum including Gaussians emission lines (see table 2), and a power-law component to represent the compact source emission. SIS-0 and SIS-1 data have been summed. Crosses denote the actual data and the histogram indicates the model. Residuals are shown in the lower panel with 1σ error bars (See tables 1 & 2 for the fitted parameters).

Plate 1 – Images of Kes 73 using data from both SIS cameras. The brightness distribution is exposure corrected and smoothed. The plots are centered on the peak (broad-band) emission and displayed on a linear scale with contours in 16 uniform increments, scaled to the image max. **Top Left** – SIS image of Kes 73 in the hard-band (2.5 - 10.0 keV); the image is consistend with an unresolved SIS point source. **Top Right** – SIS image of Kes 73 in the soft-band (0.5 - 2.5 keV); evident is a additional strong diffuse component. **Bottom Left** – The above hard-band image deconvolved using the Lucy restoration method. **Bottom Right** – The above soft-band image deconvolved using the Lucy restoration method.

Plate 2 – Decomposed SIS spectra of Kes 73. (**Upper panels**) The computed background subtracted spectrum (crosses) of the central compact source with a single absorbed power law fit (histogram). The best fit value for the photon index is 3.4. (**Bottom panels**) The computed spectrum for the thermal-nebula + background (crosses), fit with a $kT = 0.6$ keV Raymond-Smith thermal plasma model (histogram); residuals are apparent around O, Ne, and Mg. In the energy band below about 2.5 keV, the thermal component dominates, whereas the central power-law component is dominant in the harder band. The plots are shown scaled identically for ease of comparison.

Plate 2 (bottom). The Rosat HRI brightness image is overlayed with the SIS contours of the thermal emission from Kes 73 after subtracting off the non-thermal component. The method used to create this image is described in the text. The HRI image is smoothed with a boxcar filter to bring out features correlated on the same spatial scales as the contoured image.

Table 1. Spectral Models and Fit Parameters

Model	Continuum (Γ; kT)	N_H (10^{22} cm^{-2})	χ^2_ν (ν)
— The Compact Source Spectrum —			
Power-law	$3.1 - 3.7$	$2.7 - 3.4$	1.0(151)
Bremsstralung	$1.7 - 2.2$	$1.9 - 2.4$	1.0(151)
Blackbody	$0.6 - 0.7$	$1.0 - 1.4$	1.0(149)
+ power-law	$0.9 - 3.6$	–	–
— The Source + Nebular Spectrum —			
Bremss + lines	$0.5 - 0.9$	$2.1 - 2.2$	1.0(187)
+ power-law	3.4 fixed	–	–
R&S	0.6	2.9	3.2(207)
+ power-law	3.4 fixed	–	–
— Decomposed Nebular Spectrum —			
Bremss + lines	$0.6 - 0.8$	$1.6 - 2.3$	1.0(74)
R&S	$0.57 - 0.62$	$2.7 - 2.9$	3.2(88)

Fits using ASCA SIS data between $0.9 - 8.0$ keV. All continuum fits values are quoted in units of keV; all power-laws slopes are given as photon indexes $F_\nu \propto \nu^{-\Gamma}$; Raymond & Smith (R&S) fits with abundance set to 2 times cosmic. Nebular fits include 11 lines of Mg, Si, S, Ar, Ca. Gaussian line fits required $\sigma = 20$ eV. Errors are the formal 90% confidence limit for one interesting parameter.

Table 2. Measured Emission Lines in Kes 73

Line Name	Lab Energy	Line Center	Norm 10^{-3} cts/cm^2/s
O Heα	0.65	0.6±0.1	$\lesssim 0.2$
Ne Heα	0.92	0.9±0.1	$\lesssim 5$
Fe-L blends			$\lesssim 0.1$
Mg Heα . . .	1.35	1.340±0.003	4.0 ± 0.5
Mg Lyα . . .	1.48	1.47±0.05	0.14 ± 0.14
Si Heα	~ 1.86	1.848±0.003	3.1 ± 0.3
Si Lyα	2.00	1.97±0.02	0.14 ± 0.06
Si He3p+4p	~ 2.20	2.20±0.01	0.27 ± 0.04
Si Lyβ	2.38	2.37±0.03	0.25 ± 0.04
S Heα	~ 2.45	2.457±0.005	0.78 ± 0.06
S Lyα	2.62	2.64±0.14	0.05 ± 0.03
S Heβ	2.89	2.89±0.03	0.07 ± 0.03
Ar Heα	~ 3.1	3.08±0.03	0.11 ± 0.02
Ar/Ca Heα	~ 3.8	3.8±5.0	0.01 ± 0.01

A single temperature bremsstrahlung with power-law model is assumed for the continuum emission. All energies are quoted in keV. Errors are the formal 90% confidence limit for one interesting parameter. Line normalizations are given as total photons per cm^2 per sec in the line.

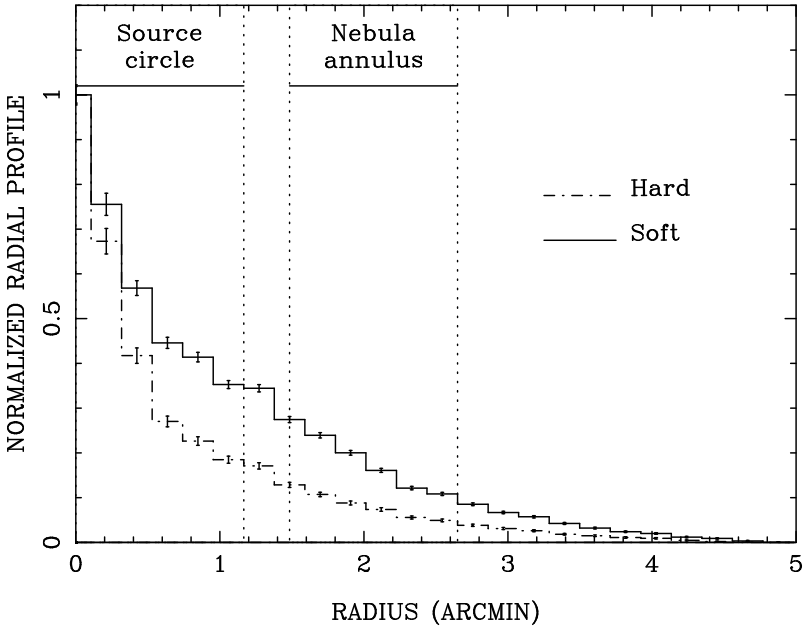
Source
circle
Nebula
annulus
Hard
Soft
NORMALIZED RADIAL PROFILE
RADIUS (ARCMIN)
0
0.5
1
0
1
2
3
4
5

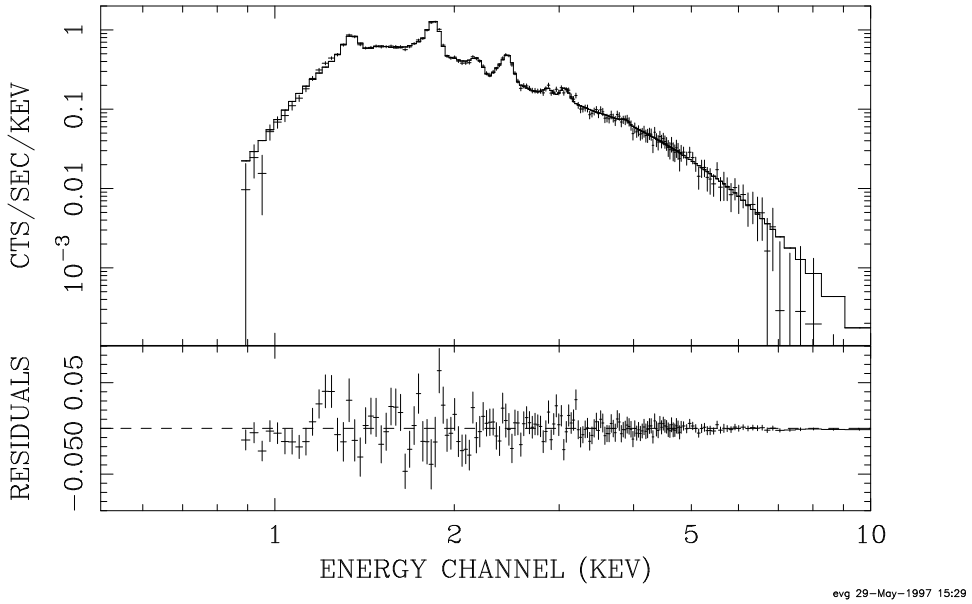
CTS/SEC/KEV
10^{-3}
0.01
0.1
1
RESIDUALS
−0.050
0.05
1
2
5
10
ENERGY CHANNEL (KEV)
evg 29−May−1997 15:29

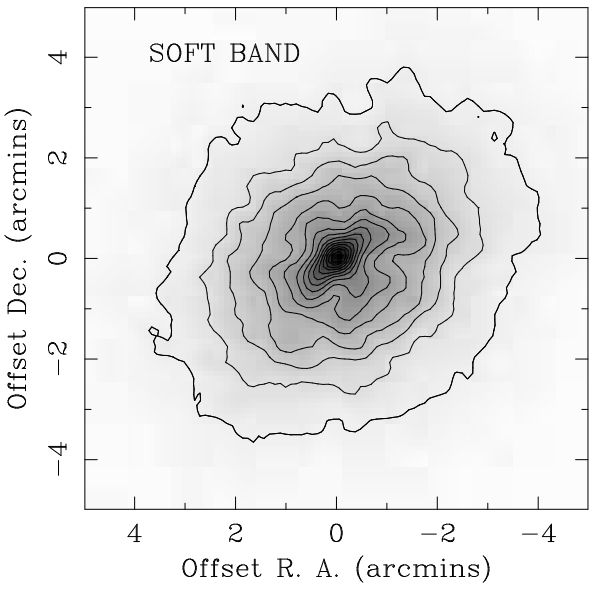
SOFT BAND
Offset Dec. (arcmins)
Offset R. A. (arcmins)
4
2
0
−2
−4

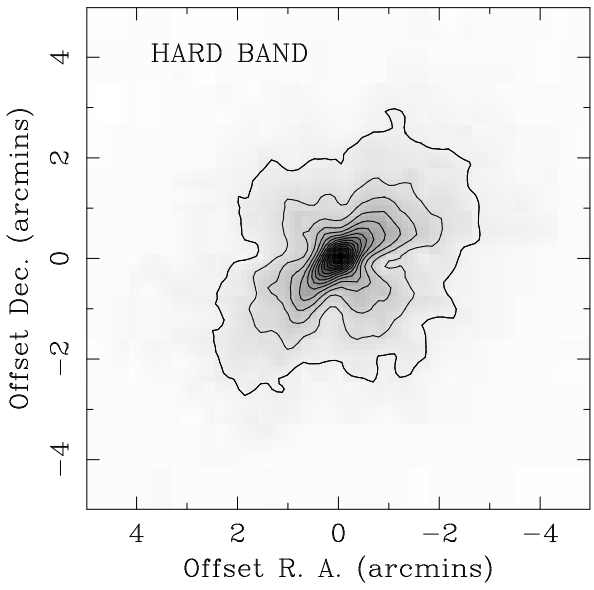
HARD BAND
Offset Dec. (arcmins)
Offset R. A. (arcmins)
4
2
0
−2
−4

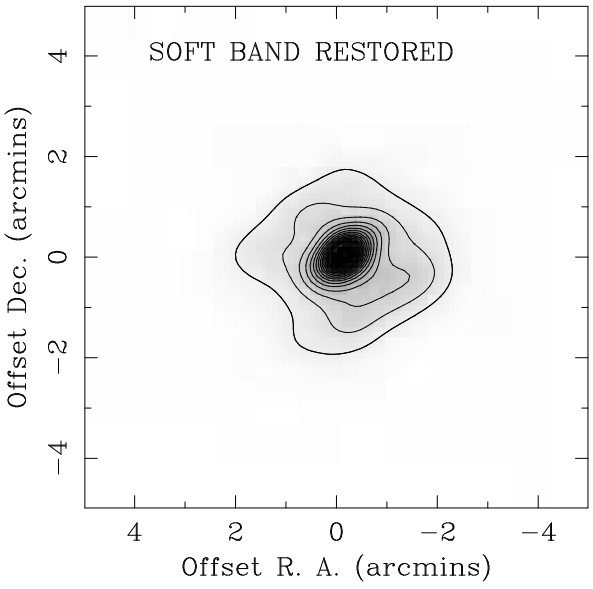
SOFT BAND RESTORED
Offset Dec. (arcmins)
Offset R. A. (arcmins)
4
2
0
−2
−4

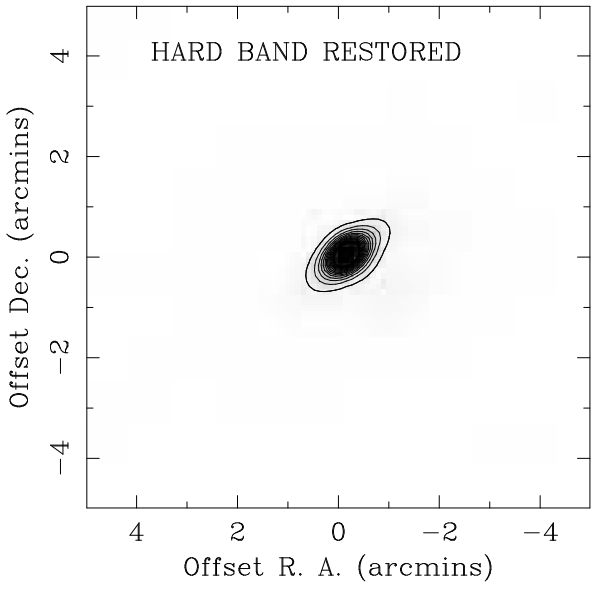
HARD BAND RESTORED
Offset Dec. (arcmins)
Offset R. A. (arcmins)
4
2
0
−2
−4

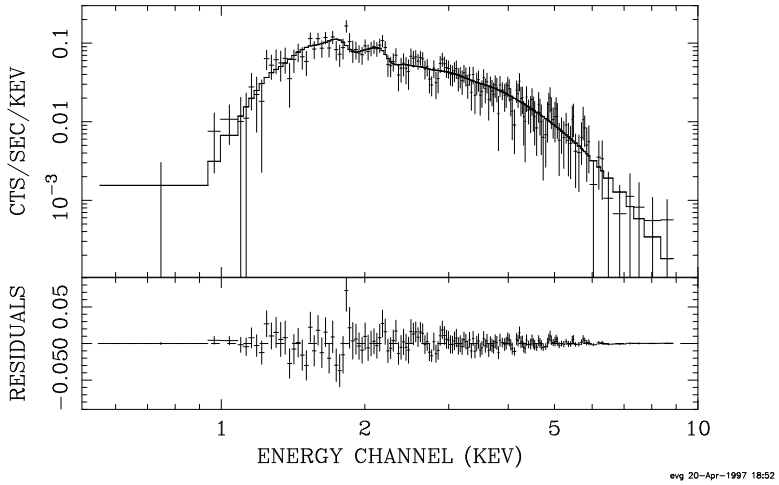
CTS/SEC/KEV
10^{-3}
0.01
0.1
RESIDUALS
−0.050 0.05
1
2
5
10
ENERGY CHANNEL (KEV)
evg 20-Apr-1997 18:52

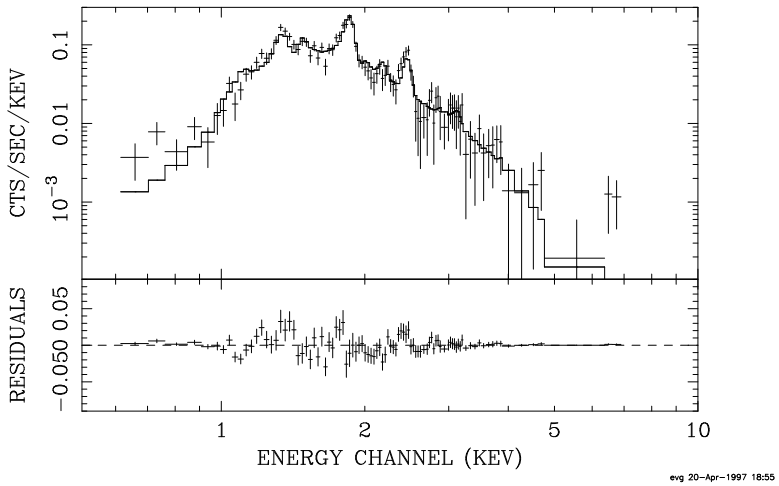
CTS/SEC/KEV
10^{-3}
0.01
0.1
RESIDUALS
−0.050 0.05
1
2
5
10
ENERGY CHANNEL (KEV)
evg 20-Apr-1997 18:55

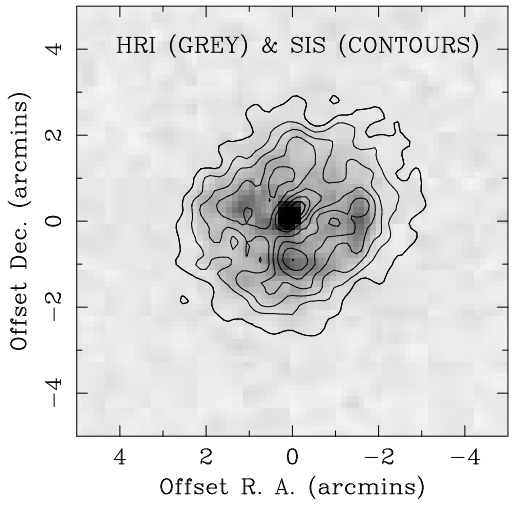
HRI (GREY) & SIS (CONTOURS)
Offset Dec. (arcmins)
4
2
0
−2
−4
Offset R. A. (arcmins)